Available online at www.sciencedirect.com
ScienceDirect
Journal of Sound and Vibration 319 (2009) 993–1002
JOURNAL OF SOUND AND VIBRATION
www.elsevier.com/locate/jsvi

Spectral element modeling for extended Timoshenko beams

Usik Lee*, Changho Lee

Department of Mechanical Engineering, Inha University, 253 Yonghyun-Dong, Nam-Gu, Incheon 402-751, Republic of Korea

Received 4 July 2007; received in revised form 23 June 2008; accepted 29 June 2008
Handling Editor: L.G. Tham
Available online 6 August 2008

Abstract

Periodic lattice structures such as the large space lattice structures and carbon nanotubes may take the extension-transverse shear-bending coupled vibrations, which can be well represented by the extended Timoshenko beam theory. In this paper, the spectrally formulated finite element model (simply, spectral element model) has been developed for extended Timoshenko beams and applied to some typical periodic lattice structures such as the armchair carbon nanotube, the periodic plane truss, and the periodic space lattice beam.

1. Introduction

In structural mechanics, the shear deformation may become important when a beam theory is applied to the beam-like lattice structures and the couplings between axial, transverse shear and bending deformations may exist when a beam-like structure is not perfectly axisymmetric along its central axis (Ref. [1]). The typical examples of such beam-like lattice structures are the beam-like space lattice structures and carbon nanotubes (CNTs). The classical Timoshenko beam theory is an extension of the Euler–Bernoulli beam theory to allow for the effects of transverse shear deformation and rotary inertia, while the extended Timoshenko beam (ETB) theory is the extension of the classical Timoshenko beam theory to take into account the couplings between axial, transverse shear and bending deformations (Ref. [2]). Thus the ETB theory is appropriate for the dynamic analysis of beam-like lattice structures.

The finite element method (FEM) is obviously a very powerful solution method which is versatile for diverse, complex engineering problems. However, as the classic finite elements are formulated by using frequency-independent simple polynomials as the interpolation functions, it is often inevitable to use extremely fine meshes to improve the accuracy of FEM solutions, especially at high frequency, which may increase the computation cost drastically, possibly with degrading the accuracy of FEM solutions. Such problems may be resolved by using frequency-dependent interpolation functions, instead of the simple polynomials, to formulate finite element models: this frequency-domain modeling method is called the spectral element method (SEM) in the literature (Ref. [3,4]). In SEM, the wave solutions satisfying governing equations

*Corresponding author. Tel.: +82 32 860 7318; fax: +82 32 866 1434.
E-mail address: ulee@inha.ac.kr (U. Lee).

0022-460X/$ - see front matter © 2008 Elsevier Ltd. All rights reserved.
doi:10.1016/j.jsv.2008.06.048

exactly in the frequency-domain are normally used as the frequency-dependent interpolation functions. Due to its intrinsic nature, SEM will provide exact frequency-domain solutions (i.e., Fourier components of dynamic responses) by using only one element for a structure of any length in the absence of any discontinuity or irregularity in geometrical and material properties, which may reduce the total degrees of freedom (dofs) to lower the computation cost and time. Thus, SEM is often referred to as an *exact* solution method (Ref. [5]). In SEM, the inverse fast Fourier transform (FFT) (Ref. [6]) is used to efficiently reconstruct the time history of the response from its Fourier components.

In the literature, spectral element models have been developed for various beam structures such as the Timoshenko beams (e.g., Ref. [7]), bending-torsion coupled beams (e.g., Ref. [8]), extension-torsion coupled beams (e.g., Ref. [9]), curved beams (e.g., Ref. [10]), twisted helix beams or springs (e.g., Ref. [11]), composite beams (e.g., Ref. [12]), active constraining layer damping treated beams (e.g., Ref. [13]), functionally graded beams (e.g., Ref. [14]), tapered beams (e.g., Ref. [15]), and so forth. To the author's best knowledge, the spectral element model for the extended Timoshenko beams (ETBs) has not been introduced in the literature.

Thus, the purposes of this paper are: (1) to develop a spectral element model for ETBs which take the extension-transverse shear-bending coupled in-plane vibrations and (2) to apply it to the beam-like lattice structures which can be homogenized as the continuum ETB models.

2. Equations of motion

The in-plane motion of an ETB is represented by (Ref. [2])

$$\begin{Bmatrix} T' \\ Q' \\ M' \end{Bmatrix} = \begin{bmatrix} \rho A & 0 & \rho R \\ 0 & \rho A & 0 \\ \rho R & 0 & \rho I \end{bmatrix} \begin{Bmatrix} \ddot{u} \\ \ddot{w} \\ \ddot{\theta} \end{Bmatrix} - \begin{Bmatrix} 0 \\ 0 \\ Q \end{Bmatrix} \tag{1}$$

where the prime ($'$) denotes the derivative with respective to the spatial coordinate, say x. T, Q, and M are the axial tensile force, transverse shear force, and bending moment, respectively; and u, w, and θ are the axial displacement, transverse displacement, and slope, respectively. ρA, ρR, and ρI are the effective mass per length, the first-order moment of inertia, and second-order moment of inertia defined by

$$\rho A = \int \rho \, \mathrm{d}A, \quad \rho R = \int \rho z \, \mathrm{d}A, \quad \rho I = \int \rho z^2 \, \mathrm{d}A \tag{2}$$

where ρ is the mass density per unit volume. The force–displacement relation is given by (Ref. [2])

$$\begin{Bmatrix} T \\ Q \\ M \end{Bmatrix} = \begin{bmatrix} EA & C_1 & C_2 \\ C_1 & GA & C_3 \\ C_2 & C_3 & EI \end{bmatrix} \begin{Bmatrix} u' \\ w' - \theta \\ \theta' \end{Bmatrix} \tag{3}$$

where C_1, C_2, and C_3 are the coupling rigidities which represent the couplings between the axial, transverse shear, and bending deformations. When all of ρR, C_1, C_2, and C_3 vanish, decoupled equations of motion for the classical Timoshenko beam and axial bar are recovered.

The ETB theory represented by Eq. (1) can be applied to the homogenized beam models of the one-dimensional-like periodic lattice structures whose cross-sections are symmetric with respect to the vertical axis (z-axis) so that they take the extension-transverse shear-bending coupled in-plane vibration in the x–z plane, without taking the torsional motion about the elastic axis (x-axis), as shown in Fig. 1.

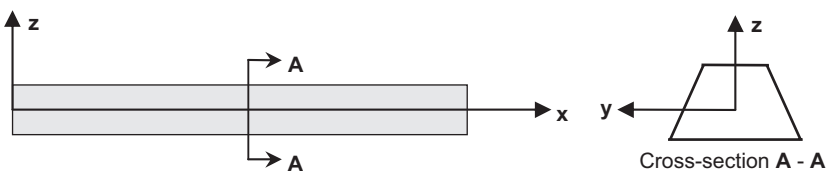

Fig. 1. The coordinates system for the extended Timoshenko beam.

3. Spectral element formulation

To formulate the spectral element of ETB, based on the discrete Fourier transform (DFT) theory (Ref. [6]), we assume the displacement fields in the spectral forms as

$$\begin{aligned} u(x,t) &= \sum_{n=0}^{N-1} \bar{u}_n(x)\, \mathrm{e}^{\mathrm{i}\omega_n t} \\ w(x,t) &= \sum_{n=0}^{N-1} \bar{w}_n(x)\, \mathrm{e}^{\mathrm{i}\omega_n t} \\ \theta(x,t) &= \sum_{n=0}^{N-1} \bar{\theta}_n(x)\, \mathrm{e}^{\mathrm{i}\omega_n t} \end{aligned} \tag{4}$$

where $\bar{u}_n, \bar{w}_n$, and $\bar{\theta}_n$ $(n = 0, 1, 2, \ldots, N-1)$ are the Fourier components of $u(x, t)$, $w(x, t)$, and $\theta(x, t)$, respectively, all corresponding to discrete frequencies defined by $\omega_n = 2\pi n/T$. The time window (period) T is related to the number of samples N by $N = 2f_{\mathrm{NYQ}}T$, where f_{NYQ} is the Nyquist frequency. Similarly we represent the axial tensile force $T(x, t)$, transverse shear force $Q(x, t)$, and bending moment $M(x, t)$ in the spectral forms as

$$\begin{aligned} T(x,t) &= \sum_{n=0}^{N-1} \bar{T}_n(x)\, \mathrm{e}^{\mathrm{i}\omega_n t} \\ Q(x,t) &= \sum_{n=0}^{N-1} \bar{Q}_n(x)\, \mathrm{e}^{\mathrm{i}\omega_n t} \\ M(x,t) &= \sum_{n=0}^{N-1} \bar{M}_n(x)\, \mathrm{e}^{\mathrm{i}\omega_n t} \end{aligned} \tag{5}$$

To shorthand, the subscript n, which indicates the nth Fourier component, will be omitted in the following derivations.

Substitution of Eqs. (4) and (5) into Eqs. (1) and (3) gives

$$\begin{Bmatrix} \bar{T}' \\ \bar{Q}' \\ \bar{M}' \end{Bmatrix} = -\omega^2 \begin{bmatrix} \rho A & 0 & \rho R \\ 0 & \rho A & 0 \\ \rho R & 0 & \rho I \end{bmatrix} \begin{Bmatrix} \bar{u} \\ \bar{w} \\ \bar{\theta} \end{Bmatrix} - \begin{Bmatrix} 0 \\ 0 \\ \bar{Q} \end{Bmatrix} \tag{6}$$

and

$$\begin{Bmatrix} \bar{T} \\ \bar{Q} \\ \bar{M} \end{Bmatrix} = \begin{bmatrix} EA & C_1 & C_2 \\ C_1 & GA & C_3 \\ C_2 & C_3 & EI \end{bmatrix} \begin{Bmatrix} \bar{u}' \\ \bar{w}' - \bar{\theta} \\ \bar{\theta}' \end{Bmatrix} \tag{7}$$

By substituting Eq. (7) into Eq. (6), one can derive the governing equations as

$$\begin{bmatrix} EA & C_1 & C_2 \\ C_1 & GA & C_3 \\ C_2 & C_3 & EI \end{bmatrix} \begin{Bmatrix} \bar{u}'' \\ \bar{w}'' \\ \bar{\theta}'' \end{Bmatrix} + \begin{bmatrix} 0 & 0 & -C_1 \\ 0 & 0 & -GA \\ C_1 & GA & 0 \end{bmatrix} \begin{Bmatrix} \bar{u}' \\ \bar{w}' \\ \bar{\theta}' \end{Bmatrix} - \begin{bmatrix} 0 & 0 & 0 \\ 0 & 0 & 0 \\ 0 & 0 & GA \end{bmatrix} \begin{Bmatrix} \bar{u} \\ \bar{w} \\ \bar{\theta} \end{Bmatrix} + \omega^2 \begin{bmatrix} \rho A & 0 & \rho R \\ 0 & \rho A & 0 \\ \rho R & 0 & \rho I \end{bmatrix} \begin{Bmatrix} \bar{u} \\ \bar{w} \\ \bar{\theta} \end{Bmatrix} = \begin{Bmatrix} 0 \\ 0 \\ 0 \end{Bmatrix} \tag{8}$$

Assume the general solutions of Eq. (8) as

$$\bar{u}(x) = \alpha W \mathrm{e}^{-\mathrm{i}kx}, \quad \bar{w}(x) = W\mathrm{e}^{-\mathrm{i}kx}, \quad \bar{\theta}(x) = \beta W \mathrm{e}^{-\mathrm{i}kx} \tag{9}$$

where k is the wavenumber. Substitution of Eq. (9) into Eq. (8) gives

$$\mathbf{X}(k)W\begin{Bmatrix} \alpha \\ 1 \\ \beta \end{Bmatrix} = \begin{Bmatrix} 0 \\ 0 \\ 0 \end{Bmatrix} \tag{10}$$

where

$$\mathbf{X}(k) = \begin{bmatrix} -k^2EA + \omega^2\rho A & -k^2C_1 & \mathrm{i}kC_1 - k^2C_2 + \omega^2\rho R \\ -k^2C_1 & -k^2GA + \omega^2\rho A & \mathrm{i}kGA - k^2C_3 \\ -k^2C_2 + \omega^2\rho R - \mathrm{i}kC_1 & -k^2C_3 - \mathrm{i}kGA & -k^2EI + \omega^2\rho I - GA \end{bmatrix} \tag{11}$$

From Eq. (10), one can obtain the dispersion equation as

$$|\mathbf{X}(k)| = a_1k^6 + a_2k^4 + a_3k^2 + a_4 = 0 \tag{12}$$

where

$$\begin{aligned} a_1 &= (C_2^2 - EAEI)GA + EIC_1^2 - 2C_1C_2C_3 + C_3^2EA \\ a_2 &= \omega^2\rho A\{EI(EA + GA) - C_2^2 - C_3^2 + 2(C_1C_3 - GAC_2)\eta_R + (EAGA - C_1^2)\eta_I\} \\ a_3 &= \omega^4\rho A^2\{EI + (EA + GA)\eta_I - 2C_2\eta_R - GA\eta_R^2\} + \omega^2\rho A(C_1^2 - EAGA) \\ a_4 &= \omega^6\rho A^3(\eta_I - \eta_R^2) - \omega^4GA\rho A^2 \\ \eta_R &= \frac{\rho R}{\rho A}, \quad \eta_I = \frac{\rho I}{\rho A} \end{aligned} \tag{13}$$

We can obtain six roots (i.e., wavenumbers) from Eq. (12) as

$$\begin{aligned} k_1 = -k_2 = \sqrt{y_1 - \frac{b_1}{3}}, \quad k_3 = -k_4 = \sqrt{y_2 - \frac{b_1}{3}}, \\ k_5 = -k_6 = \sqrt{y_3 - \frac{b_1}{3}} \end{aligned} \tag{14}$$

where

$$\begin{aligned} y_1 &= S + T, \quad y_2 = -\sqrt[3]{-1}(S + T), \quad y_3 = (-1)^{2/3}(S + T) \\ S &= \sqrt[3]{\tfrac{1}{2}(-q + \sqrt{q^2 + 4p^3})}, \quad T = \sqrt[3]{\tfrac{1}{2}(-q - \sqrt{q^2 + 4p^3})} \\ p &= \frac{3b_2 - b_1^2}{9}, \quad q = \frac{2b_1^3 - 9b_1b_2 + 27b_3}{27} \\ b_1 &= \frac{a_2}{a_1}, \quad b_2 = \frac{a_3}{a_1}, \quad b_3 = \frac{a_4}{a_1} \end{aligned} \tag{15}$$

From Eq. (10), α and β are determined as

$$\begin{aligned} \alpha &= \frac{1}{\Delta}[-\rho A\rho R\omega^4 + \{\rho R + k(-\mathrm{i}C_1\rho A + C_2k\rho A + CAk\rho R)\}\omega^2 \\ &\quad + k\{(C_1C_3 - C_2GA)k^3 + (C_3 - C_2)k + \mathrm{i}C_1 - \mathrm{i}GA\}] \\ \beta &= \frac{1}{\Delta}\{-C_1^2k^4 - C_1k^2 + (EAk^2 - \rho A\omega^2)(GAk^2 - \rho A\omega^2 + 1)\} \end{aligned} \tag{16}$$

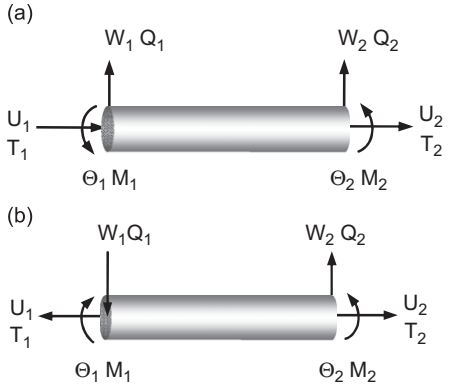

Fig. 2. Sign conventions defined for (a) the spectral element modeling and (b) the mechanics of materials.

where

$$\begin{aligned}\Delta = {} & (-\mathrm{i}C_1^2 + C_1C_2k + \mathrm{i}EAGA - C_3EAk)k^3 \\ & + (-\mathrm{i}GA\rho A + C_3k\rho A - C_1k\rho R)\omega^2 k\end{aligned} \tag{17}$$

By using the six wavenumbers computed from Eq. (14), we can express the general solutions in the forms as

$$\begin{aligned}\bar{u}(x) &= \alpha_1 W_1 \mathrm{e}^{-\mathrm{i}k_1x} + \alpha_2 W_2 \mathrm{e}^{-\mathrm{i}k_2x} + \alpha_3 W_3 \mathrm{e}^{-\mathrm{i}k_3x} + \alpha_4 W_4 \mathrm{e}^{-\mathrm{i}k_4x} + \alpha_5 W_5 \mathrm{e}^{-\mathrm{i}k_5x} + \alpha_6 W_6 \mathrm{e}^{-\mathrm{i}k_6x} \\ \bar{w}(x) &= W_1 \mathrm{e}^{-\mathrm{i}k_1x} + W_2 \mathrm{e}^{-\mathrm{i}k_2x} + W_3 \mathrm{e}^{-\mathrm{i}k_3x} + W_4 \mathrm{e}^{-\mathrm{i}k_4x} + W_5 \mathrm{e}^{-\mathrm{i}k_5x} + W_6 \mathrm{e}^{-\mathrm{i}k_6x} \\ \bar{\theta}(x) &= \beta_1 W_1 \mathrm{e}^{-\mathrm{i}k_1x} + \beta_2 W_2 \mathrm{e}^{-\mathrm{i}k_2x} + \beta_3 W_3 \mathrm{e}^{-\mathrm{i}k_3x} + \beta_4 W_4 \mathrm{e}^{-\mathrm{i}k_4x} + \beta_5 W_5 \mathrm{e}^{-\mathrm{i}k_5x} + \beta_6 W_6 \mathrm{e}^{-\mathrm{i}k_6x}\end{aligned} \tag{18}$$

or, in the simple forms as

$$\begin{aligned}\bar{u}(x) &= \mathbf{\Phi}(x)[\mathrm{diag}(\alpha_j)]\mathbf{W} \\ \bar{w}(x) &= \mathbf{\Phi}(x)\mathbf{W} \qquad (j = 1,2,3,4,5,6) \\ \bar{\theta}(x) &= \mathbf{\Phi}(x)[\mathrm{diag}(\beta_j)]\mathbf{W}\end{aligned} \tag{19}$$

where

$$\begin{aligned}\mathbf{\Phi}(x) &= [\,\mathrm{e}^{-\mathrm{i}k_1x} \quad \mathrm{e}^{-\mathrm{i}k_2x} \quad \mathrm{e}^{-\mathrm{i}k_3x} \quad \mathrm{e}^{-\mathrm{i}k_4x} \quad \mathrm{e}^{-\mathrm{i}k_5x} \quad \mathrm{e}^{-\mathrm{i}k_6x}\,] \\ \mathbf{W} &= \{\,W_1 \quad W_2 \quad W_3 \quad W_4 \quad W_5 \quad W_6\,\}^{\mathrm{T}} \\ \alpha_j &= \alpha(k_j), \quad \beta_j = \beta(k_j)\end{aligned} \tag{20}$$

The Fourier components of the dof and the nodal forces and moments, shown in Fig. 2, are defined by

$$\begin{aligned}\mathbf{d} &= \{\,U_1 \quad W_1 \quad \Theta_1 \quad U_2 \quad W_2 \quad \Theta_2\,\}^{\mathrm{T}} \\ &= \{\,\bar{u}(0) \quad \bar{w}(0) \quad \bar{\theta}(0) \quad \bar{u}(L) \quad \bar{w}(L) \quad \bar{\theta}(L)\,\}^{\mathrm{T}}\end{aligned} \tag{21}$$

$$\begin{aligned}\mathbf{f} &= \{\,T_1 \quad Q_1 \quad M_1 \quad T_2 \quad Q_2 \quad M_2\,\}^{\mathrm{T}} \\ &= \{\,-\bar{T}(0) \quad -\bar{Q}(0) \quad -\bar{M}(0) \quad \bar{T}(L) \quad \bar{Q}(L) \quad \bar{M}(L)\,\}^{\mathrm{T}}\end{aligned} \tag{22}$$

Substitution of Eq. (19) into Eq. (21) yields the relation as

$$\mathbf{d} = \mathbf{H}(\omega)\mathbf{W} \tag{23}$$

where

$$\mathbf{H}(\omega)=\begin{bmatrix} \alpha_1 & \alpha_2 & \alpha_3 & \alpha_4 & \alpha_5 & \alpha_6 \\ 1 & 1 & 1 & 1 & 1 & 1 \\ \beta_1 & \beta_2 & \beta_3 & \beta_4 & \beta_5 & \beta_6 \\ \alpha_1\varepsilon_1 & \alpha_2\varepsilon_2 & \alpha_3\varepsilon_3 & \alpha_4\varepsilon_4 & \alpha_5\varepsilon_5 & \alpha_6\varepsilon_6 \\ \varepsilon_1 & \varepsilon_2 & \varepsilon_3 & \varepsilon_4 & \varepsilon_5 & \varepsilon_6 \\ \beta_1\varepsilon_1 & \beta_2\varepsilon_2 & \beta_3\varepsilon_3 & \beta_4\varepsilon_4 & \beta_5\varepsilon_5 & \beta_6\varepsilon_6 \end{bmatrix} \tag{24}$$

$$\varepsilon_j=\mathrm{e}^{-\mathrm{i}k_jL} \quad (j=1,2,\ldots,6) \tag{25}$$

By using Eq. (23), Eq. (19) can be rewritten as

$$\begin{aligned} \bar{u}(x)&=\mathbf{N}_U(x;\omega)\mathbf{d} \\ \bar{w}(x)&=\mathbf{N}_W(x;\omega)\mathbf{d} \\ \bar{\theta}(x)&=\mathbf{N}_\Theta(x;\omega)\mathbf{d} \end{aligned} \tag{26}$$

where $\mathbf{N}_U$, $\mathbf{N}_W$, and $\mathbf{N}_\Theta$ are the frequency-dependent shape functions defined by

$$\begin{aligned} \mathbf{N}_U(x;\omega)&=\mathbf{\Phi}(x)[\mathrm{diag}(\alpha_j)]\mathbf{H}^{-1} \\ \mathbf{N}_W(x;\omega)&=\mathbf{\Phi}(x)\mathbf{H}^{-1} \\ \mathbf{N}_\Theta(x;\omega)&=\mathbf{\Phi}(x)[\mathrm{diag}(\beta_j)]\mathbf{H}^{-1} \end{aligned} \tag{27}$$

Substitution of Eq. (26) into Eq. (7) and its result into Eq. (22) gives the relation between the nodal force and moment vector $\mathbf{f}$ and the nodal dof vector $\mathbf{d}$ as

$$\mathbf{f}=\mathbf{S}(\omega)\mathbf{d} \tag{28}$$

where $\mathbf{S}(\omega)$ is the frequency-dependent dynamic stiffness matrix, often called spectral element matrix, given by

$$\mathbf{S}(\omega)=\begin{bmatrix} \mathbf{R} & \mathbf{0} \\ \mathbf{0} & \mathbf{R} \end{bmatrix}\mathbf{\Psi}\mathbf{H}^{-1} \tag{29}$$

where $\mathbf{0}$ is the zero matrix, and $\mathbf{R}$ and $\mathbf{\Psi}$ are defined by

$$\mathbf{R}=\begin{bmatrix} EA & C_1 & C_2 \\ C_1 & GA & C_3 \\ C_2 & C_3 & EI \end{bmatrix} \tag{30}$$

$$\mathbf{\Psi}=\begin{bmatrix} \mathrm{i}k_1\alpha_1 & \mathrm{i}k_2\alpha_2 & \mathrm{i}k_3\alpha_3 & \mathrm{i}k_4\alpha_4 & \mathrm{i}k_5\alpha_5 & \mathrm{i}k_6\alpha_6 \\ \chi_1 & \chi_2 & \chi_3 & \chi_4 & \chi_5 & \chi_6 \\ \mathrm{i}k_1\beta_1 & \mathrm{i}k_2\beta_2 & \mathrm{i}k_3\beta_3 & \mathrm{i}k_4\beta_4 & \mathrm{i}k_5\beta_5 & \mathrm{i}k_6\beta_6 \\ -\mathrm{i}k_1\alpha_1\varepsilon_1 & -\mathrm{i}k_2\alpha_2\varepsilon_2 & -\mathrm{i}k_3\alpha_3\varepsilon_3 & -\mathrm{i}k_4\alpha_4\varepsilon_4 & -\mathrm{i}k_5\alpha_5\varepsilon_5 & -\mathrm{i}k_6\alpha_6\varepsilon_6 \\ -\chi_1\varepsilon_1 & -\chi_2\varepsilon_2 & -\chi_3\varepsilon_3 & -\chi_4\varepsilon_4 & -\chi_5\varepsilon_5 & -\chi_6\varepsilon_6 \\ -\mathrm{i}k_1\beta_1\varepsilon_1 & -\mathrm{i}k_2\beta_2\varepsilon_2 & -\mathrm{i}k_3\beta_3\varepsilon_3 & -\mathrm{i}k_4\beta_4\varepsilon_4 & -\mathrm{i}k_5\beta_5\varepsilon_5 & -\mathrm{i}k_6\beta_6\varepsilon_6 \end{bmatrix} \tag{31}$$

where

$$\chi_j=\mathrm{i}k_j+\beta_j \quad (j=1,2,\ldots,6) \tag{32}$$

The spectral element Eq. (28) can be assembled in an analogous way as used in the conventional finite element method. After applying the relevant boundary conditions, a global dynamic stiffness matrix equation can be

obtained in the form as

$$\mathbf{f}_g = \mathbf{S}_g(\omega)\mathbf{d}_g \tag{33}$$

where the subscript g denotes the quantities for an assembled global ETB system.

4. Spectral element analysis

As the global dynamic stiffness matrix $\mathbf{S}_g(\omega)$ exactly relates the spectral dofs with the spectral nodal forces and moments at a frequency ω, one can use only one element to model an ETB structure of any length in the absence of any discontinuity or irregularity in geometrical and material properties.

The natural frequencies ω_{NAT} of a global system can be computed from the condition that the determinant of the global dynamic stiffness matrix vanishes at ω_{NAT}. That is

$$\det \mathbf{S}_g(\omega_{\mathrm{NAT}}) = 0 \tag{34}$$

To compute the roots (i.e., natural frequencies ω_{NAT}) of Eq. (34), we can use a proper root finding algorithm together with using the Wittrick–William algorithm (Ref. [16]) not to miss any roots within a frequency range specified during the root search.

The spectral nodal dofs can be exactly computed from Eq. (31) as

$$\mathbf{d}_g = \mathbf{S}_g(\omega)^{-1}\mathbf{f}_g = \mathbf{T}_g(\omega)\mathbf{f}_g \tag{35}$$

where $\mathbf{T}_g(\omega) = \mathbf{S}_g(\omega)^{-1}$ is the system transfer matrix or the frequency response function. Thus, Eq. (34) implies that the spectral nodal DOFs can be computed by convolving the system transfer matrix with the spectral nodal forces and moments. Lastly we use the inverse FFT to compute the time history of the response.

5. Applications

Before the application of the present spectral element model, we first evaluate its high accuracy by comparing the natural frequencies of an ETB obtained by using the spectral element model with those obtained by using the conventional finite element model. We have considered an ETB that was considered in Ref. [19]. The ETB has the length of 1 m and its material properties are given by

$$\begin{aligned} EA &= 20.3\times10^6\,\mathrm{N}, & GA &= 0.66\times10^6\,\mathrm{N}, & EI &= 11.70\times10^6\,\mathrm{N\,m^2}\\ C_1 &= 0.99\times10^6\,\mathrm{N}, & C_2 &= 17.90\times10^6\,\mathrm{N\,m}, & C_3 &= 0.00\,\mathrm{N\,m}\\ \rho A &= 0.96\,\mathrm{kg/m}, & \rho R &= -0.69\,\mathrm{kg}, & \rho I &= 5.01\,\mathrm{kg\,m} \end{aligned}$$

We have used the finite element model developed in the author's previous work (Ref. [2]) and the results are shown in Table 1 for two boundary conditions: clamped–free boundary and simply–simply supported

Table 1
Comparison of the natural frequencies computed by the present spectral element model and the finite element model

Boundary Conditions	Mode Number	FEM(n)						SEM
		$n=3$	$n=5$	$n=10$	$n=20$	$n=50$	$n=100$	$n=1$
Clamped–free	1st	226.9	224.9	224.0	223.8	223.6	223.6	223.6
	3rd	1291	1183	1100	1079	1073	1072	1072
	5th	4708	1773	1576	1519	1503	1500	1499
Simply–simply supported	1st	57.78	57.77	57.77	57.77	57.77	57.77	57.77
	3rd	884.5	854.4	828.2	820.8	818.8	818.5	818.3
	5th	3443	1479	1344	1308	1298	1297	1296

Note: FEM(n) denotes the finite element analysis results obtained by using n finite elements.

boundary. It is obvious from Table 1 that the natural frequencies obtained by using the finite element model converge to the results obtained by using the spectral element model as the number of finite elements used for finite element analysis is increased. This confirms that the spectral element model indeed provides extremely accurate solutions as many researchers (e.g., Ref. [3–5,11]) have already recognized the spectral element method as an exact element method.

For the application of the present SEM model, we consider a carbon nanotube, a plane truss, and a space lattice beam as example lattice structures. As the cross sections of the example lattice structures considered in this study are all symmetric with respect to the plane in which they vibrate, the example lattice structures can be considered to take the in-plane motion only without the torsional mode about their elastic axes. In the previous studies (e.g., Ref. [2,18]), the example lattice structures were homogenized as the equivalent continuum ETB models. Accordingly we apply the present SEM model to the homogenized continuum ETB models to investigate the natural frequencies of example lattice structures.

5.1. Carbon nanotubes

Fig. 3(a) shows an armchair single-walled carbon nanotube (SWCNT) together with its repeating cell. The geometry of SWCNT is denoted by the chirality vector (n, n), where n is the integer index (Ref. [17]). The effective structural rigidities and mass inertia properties of the armchair SWCNT (5, 5) represented by a homogenized continuum ETB model are given in Ref. [18]:

$$EA = 762.23\,\text{kg nm/s}^2, \quad GA = 674.65\,\text{kg nm/s}^2, \quad EI = 44.306\,\text{kg nm}^3/\text{s}^2$$
$$C_1 = 0\,\text{kg nm/s}^2, \quad C_2 = 0\,\text{kg nm/s}^2, \quad C_3 = 0\,\text{kg nm/s}^2$$
$$\rho A = 1.6217 \times 10^{-24}\,\text{kg/nm}, \quad \rho R = 0\,\text{kg}, \quad \rho I = 9.3184 \times 10^{-26}\,\text{kg nm}$$

The present spectral element model is applied to the CNTs (5, 5) with fifty RCUs (i.e., total length is 12.29 nm) to evaluate their natural frequencies when they are subjected to the clamped–free (cantilevered) boundary condition and the simply–simply supported boundary condition. The results are displayed in Table 2.

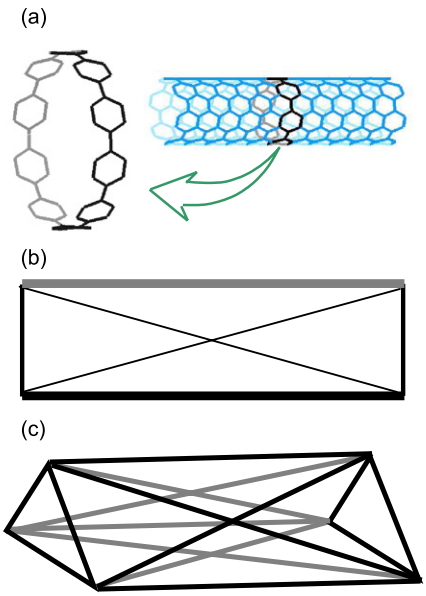

Fig. 3. Example periodic lattice structures: the repeating cells of (a) armchair single-walled carbon nanotube, (b) periodic plane truss, and (c) periodic space lattice beam.

Table 2
Natural frequencies of the armchair single-walled carbon nanotubes (5, 5)

Boundary conditions	Natural frequency (GHz)				
	ω_1	ω_2	ω_3	ω_4	ω_5
Clamped–free	19.3	119.7	329.3	440.7	630.1
Simply–simply supported	54.1	213.8	440.7	772.2	819.1

Table 3
Natural frequencies of a periodic plane truss

Boundary conditions	Natural frequency (Hz)				
	ω_1	ω_2	ω_3	ω_4	ω_5
Clamped–free	0.30	1.76	4.42	7.53	10.77
Simply–simply supported	0.96	3.36	6.39	9.59	12.81

Table 4
Natural frequencies of a periodic space lattice beam

Boundary conditions	Natural frequency (Hz)				
	ω_1	ω_2	ω_3	ω_4	ω_5
Clamped–free	0.66	3.80	9.52	12.97	16.44
Simply–simply supported	1.82	6.67	12.54	13.63	20.95

5.2. Periodic plane truss

Fig. 3(b) shows the repeating cell isolated from a typical plane truss with 20 repeating cells. All lattice members within a repeating cell (i.e., one upper longitudinal bar, one lower longitudinal bar, one diagonal bar, and two battens) are made of same material, which has the mass density $2768\,\mathrm{kg/m^3}$ and Young's modulus $71.7\times10^9\,\mathrm{N/m^2}$. The lengths of the longitudinal bar, diagonal bar, and batten are 7.5, 9.0, and 5.0 m, respectively. The cross-sectional areas of the upper longitudinal bar, lower longitudinal bar, diagonal bar, and batten are 8×10^{-5}, $18\times10^{-5}\,\mathrm{m^2}$, 4×10^{-5}, and 6×10^{-5}, respectively, and the effective structural properties for the homogenized continuum ETB model of the periodic plane truss are given in (Ref. [2]):

$$EA = 20.30\times10^6\,\mathrm{N},\quad GA = 0.73\times10^6\,\mathrm{N},\quad EI = 11.70\times10^6\,\mathrm{N\,m^2}$$
$$C_1 = 1.10\times10^6\,\mathrm{N},\quad C_2 = -17.90\times10^6\,\mathrm{N\,m},\quad C_3 = 0\,\mathrm{N\,m}$$
$$\rho A = 0.96\,\mathrm{kg/m},\quad \rho R = -0.69\,\mathrm{kg},\quad \rho I = 5.01\,\mathrm{kg\,m}$$

Table 3 shows the natural frequencies obtained by applying the present spectral element model to the periodic plane truss with 20 repeating cells (i.e., total length is 150 m) when it is subjected to clamped–free boundary condition and the simply–simply supported boundary condition.

5.3. Periodic space lattice beam

Fig. 3(c) shows the repeating cell for a typical three-dimensional lattice beam with ten repeating cells, which has been proposed for space applications. The length of a repeating cell unit is 7.5 m and the details of the material properties and geometric dimensions of the lattice elements within the repeating cell are given in (Ref. [2]). The effective structural properties for the homogenized continuum ETB model of the periodic space

lattice beam are given as (Ref. [2]):

$$EA = 2.71 \times 10^7\ \text{N}, \quad GA = 0.22 \times 10^7\ \text{N}, \quad EI = 9.61 \times 10^7\ \text{N m}^2$$
$$C_1 = 0\ \text{N}, \quad C_2 = -1.96 \times 10^7\ \text{N m}, \quad C_3 = 0\ \text{N m}$$
$$\rho A = 1.79\ \text{kg/m}, \quad \rho R = -1.30\ \text{kg}, \quad \rho I = 6.06\ \text{kg m}$$

Similarly the present spectral element model is applied to the cantilevered plane truss with 20 repeating cells (i.e., total length is 75 m) to evaluate its natural frequencies when it is subjected to the clamped–free boundary condition and the simply–simply supported boundary condition. The results are given in Table 4.

6. Conclusions

In this paper, we have developed a spectral element model for the extended Timoshenko beams for the applications to some typical periodic, beam-like lattice structures which may take extension-transverse shear-bending coupled vibrations. The spectral element model has been formulated by using the variational approach of finite element formulation. The wave solutions analytically solved to satisfy the governing equations of motion in the frequency-domain have been used as the frequency-dependent interpolation functions. Lastly, the spectral element model has been applied to the homogenized continuum ETB models of some example lattice structures such as the armchair carbon nanotube, periodic plane truss, and the periodic space lattice beam to evaluate their natural frequencies.

Acknowledgment

This work was supported by Inha University Research Grant.

References

[1] H.L. Langhaar, *Energy Methods in Applied Mechanics*, Wiley, New York, 1962.
[2] U. Lee, Dynamic continuum modeling of beamlike space structures using finite-element matrices, *AIAA Journal* 28 (4) (1990) 725–731.
[3] J.F. Doyle, *Wave Propagation in Structures: Spectral Analysis using Fast Discrete Fourier Transforms*, Springer, New York, 1997.
[4] U. Lee, *Spectral Element Method in Structural Dynamics*, Inha University Press, Inha University, Incheon, Korea, 2004.
[5] J.R. Banerjee, Dynamic stiffness formulation for structural elements: a general approach, *Computers & Structures* 63 (1) (1997) 101–103.
[6] D.E. Newland, *Random Vibrations, Spectral and Wavelet Analysis*, Longman, New York, 1993.
[7] W.P. Howson, F.W. Williams, Natural frequencies of frames with axially loaded Timoshenko members, *Journal of Sound and Vibration* 26 (1973) 503–515.
[8] P.O. Friberg, Coupled vibration of beams-an exact dynamic element stiffness matrix, *International Journal for Numerical Methods in Engineering* 19 (1983) 479–493.
[9] J.R. Banerjee, F.W. Williams, An exact dynamic stiffness matrix for coupled extensional-torsional vibration of structural members, *Computers & Structures* 50 (1994) 161–166.
[10] M.S. Issa, Natural frequencies of continuous curved beams on Winkler-type foundation, *Journal of Sound and Vibration* 127 (1988) 291–310.
[11] A.Y.T. Leung, Exact stiffness matrix for twisted helix beam, *Finite Elements in Analysis and Design* 9 (1991) 23–32.
[12] M. Eisenberger, H. Abramovich, O. Shulepov, Dynamic stiffness analysis of laminated beams using a first order shear deformation theory, *Computers & Structures* 31 (1995) 265–271.
[13] U. Lee, J. Kim, Spectral element modeling for the beams treated with active constraining layer damping, *International Journal of Solids and Structures* 38 (32–33) (2001) 5679–5702.
[14] A. Chakraborty, S. Gopalakrishnan, A spectrally formulated finite element for wave propagation analysis in functionally graded beams, *International Journal of Solids and Structures* 40 (10) (2003) 2421–2448.
[15] J.R. Banerjee, F.W. Williams, Exact Bernoulli-Euler dynamic stiffness matrix for a range of tapered beams, *International Journal for Numerical Methods in Engineering* 21 (12) (2005) 2289–2302.
[16] W.H. Wittrick, F.W. Williams, A general algorithm for computing natural frequencies of elastic structures, *Quarterly Journal of Mechanics and Applied Mathematics* 24 (1971) 263–284.
[17] M.S. Dresselhaus, G. Dresselhaus, R. Saito, Physics of carbon nanotubes, *Carbon* 33 (7) (1995) 883–891.
[18] U. Lee, H. Oh, Evaluation of the structural properties of single-walled carbon nanotubes by using a dynamic continuum modeling method, *Mechanics of Advanced Materials and Structures* 15 (2) (2008) 79–87.
[19] C.T. Sun, B.J. Kim, T.L. Bogdanoff, On the derivation of equivalent simple models for beam- and plate-like structures in dynamic analysis, AIAA Paper 81-0624, April 1981, pp. 523–532.